Mechanics of Jointed and Faulted Rock, Rossmanith (ed.) © 1990 Balkema, Rotterdam. ISBN 90 6191 155 9

Towards 3-D modelling of inelastic deformation around deep-level mines

S. M. Spottiswoode
Rock Engineering Division, COMRO, Johannesburg, South Africa

ABSTRACT
Mining in deep-level, hard-rock mines seems inevitably to lead to seismicity and resulting rockburst damage. Currently, planning of mine layouts in South African deep-level gold mines is based on models assuming elastic behaviour of the rock mass : either the elastic strain energy changes are considered or slip is modelled on discrete fault planes to provide estimates of potential seismicity.

This paper presents a two-dimensional, continuum plane-strain numerical model in which the assumption of rock-mass elasticity is relaxed through sets of potential shear zones or through failure of the rock-mass wherever its strength is exceeded. A strain-discontinuity approach, a Boundary Element method, is used, with Fast Fourier Transforms being used for rapid calculation of stresses from inelastic strains. A model of a typical mining situation shows pervasive deviations from elastic behaviour in qualitative and quantitative agreement with underground observations. While further insight will be obtained from studies in two-dimensions, a fully three-dimensional model will be needed for planning in practical mining situations. This model has been partially developed.

1 INTRODUCTION

Rockbursts and rockfalls account for about 50 percent of fatalities in the South African gold mines, with rockbursts becoming increasingly important at depths greater than 2000 metres below surface (Anon, 1988). Although good local support reduces rockfalls greatly, a strategic approach is also used to limit seismicity near working faces by following planned mine layouts. This approach typically results in leaving stabilising pillars or bracket pillars on dykes or faults, based on the criteria of Energy Release Rate, the spatial rate of energy release (ERR) or Excess Shear Stress (ESS) (Ryder, 1988).

ERR is closely related to the volume of stope closure and reduction of stope closure has been used for strategic mine planning. For example, stabilising pillars have been used since the 1960's and McGarr and Wiebols (1977) showed that seismicity was directly proportional to the volume of elastic closure in one area, with pillars reducing seismicity by some 70 percent. The volume of closure is generally estimated in terms of ERR along advancing faces and ERR is currently the most commonly used criterion for designing mine layouts to reduce rockbursts.

As the larger seismic events, those with Richter Magnitude (M) greater than 2, involve failure of rock extending for 50 metres and more from mining excavations (Spottiswoode, 1984, Lenhardt, 1989), ERR based on deformation on the reef plane cannot be expected

to account for the total amount of deformation and another approach is needed to model this situation. Ryder (1988) proposed the Excess Shear Stress model for accounting for the deformation associated with larger seismic events on faults. In this model shear slip takes place to limit shear stress, τ, to $\tau = \mu.\sigma_n$, where μ and σ_n are respectively the coefficient of friction and normal stress acting on the fault. This is the standard Coulomb failure criterion with zero cohesive strength. Ryder (1988) suggested using $\mu = 0.6$. The MINSIM-D computer program (Ryder and Napier, 1985) was used for this work and can model mining on several reef planes and on one or more slip planes in a pseudo three-dimensional approach.

Webber (1990) has applied this model in an attempt to back-analyse several large fault-related seismic events. He found that the predicted event magnitude is very sensitive to the presence and position of small unmined blocks of ground, or remnants, as well as to changes in the frictional properties on the fault and to virgin stress conditions. Although ESS studies are prone to these errors, they have demonstrated that explicit modelling within three spatial dimensions is practical and can generate sufficient inelastic deformation to account for the total level of seismicity.

2 ROCK MASS MODELLING : THE INVERSE PROBLEM

The deformations associated with seismicity around South African deep-level gold mines occur on scales ranging from remnant sizes to maximum stope spans, say from ten metres to a kilometre. Ideally any such models should allow the rock to fail and deform wherever its strength is exceeded. The prediction of deformation from known rock conditions is called the FORWARD PROBLEM.

However, rock stresses and

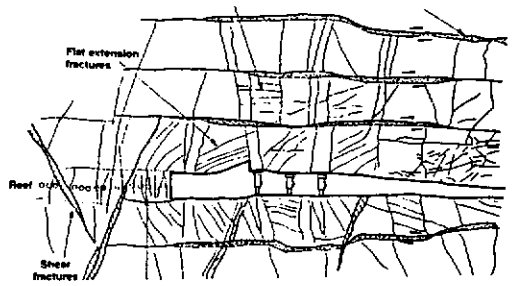

Fig. 1 Diagram showing fracturing around a deep-level stope (From Anon, 1988)

properties vary from point to point in a way that cannot be accurately predicted without measurable deformation taking place. The ideal model will therefore, in the long term, also need to be continuously adjusted to account for observed aseismic and seismic deformations. It will address the INVERSE PROBLEM by searching for spatial variations in rock stresses and properties. The forward model will be severely tested by its application to the inverse model. Considerable insight will be needed for such a model to provide more than just wisdom after the fact. Problems with non-uniqueness and numerical instabilities will be avoided by careful choice of constraints. Briefly :

1. Constitutive laws are needed for all mining situations. Failure and post-failure deformation subject to increasing stresses are reasonably well understood. However, mining can change the stress conditions around advancing faces such that fractures are formed and mobilised at a variety of different angles at different times, as can be inferred from Figure 1.

2. As little is known about local variations in virgin stress, the stress field is usually assumed to be constant over regional scales. In the South African gold mines, for example, the maximum principal stress is usually taken as vertical and equal to the overburden pressure, while horizontal stresses

are assumed to be isotropic and half of the vertical stresses. Laws of continuity of force provide some real-world restraints to variations is stresses associated with geological features (Gay, 1979).

3. Rock properties are strongly controlled by rock types, sedimentary or igneous, and can therefore be extrapolated over considerable distances. The friction properties on faults are unlikely to be constant, but might vary with country rock and with fault complexity. Time-dependent factors could be included to account for creep.

We will only be able to say that we understand the in-situ behaviour of the mechanics of jointed rock around deep-level, hard-rock mines when we find solutions to the inverse problem. Only the most comprehensive models will be useful for the inverse problem.

3 THREE DIMENSIONAL INELASTIC DEFORMATION AND MODELLING

Mandelbrot (1983) argued for the use of fractal dimensions for describing a variety of natural phenomena that have effective dimensions less than their physical dimensions by a value less than one. An example is that of fractal dimensions of coast-lines that can vary from 1.0 for a smooth coastline to 1.25 for a more convoluted coastline. Part of the beauty of fractal shapes is that they are scale invariant at a range of sizes. In this section, it will be argued that inelastic deformations around deep mines have fractal dimensions that range from 2 to 3. Two-dimensional (2-D) problems on a small number of discrete cracks are well solved using Boundary Elements, while a 3-D continuum approach is usually modelled using Finite Elements or Discrete Elements methods.

Deformations around mining, or stoping, of extensive tabular ore-bodies within purely elastic rock can be modelled very accurately and efficiently using Displacement Discontinuity (DD) elements placed within the mined-out area (Crouch and Starfield, 1983). Very complex mining patterns on single planar reefs can be studied using microcomputers (Spottiswoode, 1990). While elastic behaviour of the entire rock-mass in three dimensions is considered, the problem has been reduced to a two-dimensional (2-D) problem by approximating the stoping by an infinitesimally thin slit.

Single planar reefs are somewhat exceptional in mining as faulting and multiple reefs are common and it is often convenient to consider mining as taking place on a small number of discrete planes, each of which extend several hundred metres in all directions. As the DD elements are still planar, the numerical problem can still be viewed as 2-D. On the other hand, inelastic behaviour on the reef horizons now extends outside any single plane and these models also have some claim to solving 3-D numerical problems, although only for elastic behaviour. As the reef planes have similar sizes, the fractal dimension of multi-reef simulations is still 2.

The smallest dimension of mining in massive ore bodies can usually not be ignored and elastic behaviour can be modelled by placing DD's or Force Discontinuities around the mined-out volume. Again, these elements are 2-D within a 3-D environment. Finite Element and Finite Difference models are used to solve for rock deformation using a plastic continuum for modelling, for example, failure of high-stressed remnants or corners or the deformation of backfill. Some of these models are solving fully 3-D problems, whereas others should be viewed as perhaps 2.5-D systems. This paper presents some progress towards a 3-D model using the extended Boundary Element method adapted by Peirce and Ryder (1983) from work done by Bannerjee and Cathie (1979) and others.

Why do we need a 3-D rock-mass

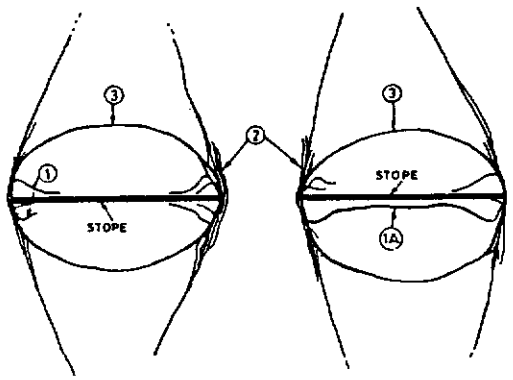

Fig. 2 Fracturing associated with isolated pillars (from Ozbay and Ryder, 1989)

modeller for extensive tabular mining? Would it not be simpler and more efficient to extend the MINSIM-D explicit slip approach to cover an adequate number of slip planes (Webber, 1990), to develop better models that look at stresses in more detail within an elastic rock mass (Spottiswoode, 1988) or to combine these approaches. It is argued here that rock deformation is more complex than is allowed for in most previous studies as inelastic deformation of the rock mass is EXTENSIVE, INTENSIVE and PERVASIVE.

Rock failure EXTENDS for distances of the same order as the mining spans, preferentially on geological faults, but also in previously intact rock as shown in Figure 2, drawn by Ozbay and Ryder (1989) from a section through a laboratory sample of homogeneous rock tested to failure. Spottiswoode (1984, 1988) found that many seismic events ahead of an advancing longwall located 50m from reef and that total seismicity could be reasonably well modelled using stresses at 50m from reef. Certainly, then, stress effects extend widely.

McGarr (1976) investigated the sum of seismic moments ΣM_o as a function of the volume of elastic closure (ΔV_e) and proposed the relationship

$$\gamma = \frac{\Sigma M_o}{G \Delta V_e}$$

where γ is a constant close to one and G is the modulus of rigidity. γ can be viewed as the total "volume of ride" (Ryder, 1988) divided by the volume of elastic closure. McGarr (1976), McGarr and Wiebols (1977) and Spottiswoode (1990) have reported values close to one. Fracturing, therefore, not only extends widely, but is also sufficiently INTENSIVE to account for the measured volumes of ride, even allowing for possible errors in seismic moment calculations (Brummer and Rorke, 1990). McGarr (1986) proposed that γ is a function of variations in rock types. Constant γ implies that seismicity per area mined is proportional to ERR. For non-zero values of γ, the closure will generally be greater than predicted by elastic theory and some value other than ΔV_e should be used to represent the influence of mining. Movement on the fractures shown in Figure 1 is also sufficiently intense that stope closure typically takes place several times faster than expected from elastic theory.

The word PERVASIVE is used here to indicate that rock fractures are both too numerous and too non-planar to be well modelled by discrete planes, particularly during remnant extraction. The Figure 1 shows the pervasive rock fracturing typically observed within some 10 metres of advancing faces. Ortlepp (1978) observed mining-induced shear fractures spaced some 30m apart at 20m below the reef during extraction of a large remnant. Such observations are rarely reported because, as stresses decrease with increasing distance from faces and abutments, so geological features are exploited preferentially and recent shear slip on faults and dyke contacts is often difficult to measure or even to identify. However, even a large number of discrete, closely-spaced fractures

do not warrant a fully 3-D approach.

The pattern of discrete planar fractures changes to that of a fracture zone where planes intersect at (2) in Figure 2, as seen more clearly in the original sample. Lenhardt (1989) studied aftershocks of seismic events associated with pillar foundation failure and failure of an abutment edge. He found that pillar failure resulted in a failure zone extending a pillar width (3[illegible] m) below the pillar, with a solid core around the centre of the pillar. Legge and Spottiswoode (1987) followed Aki (1981) in interpreting an increase of seismic b-values during remnant extraction from 1.0 to 1.5 as volumetric rather than planar distribution of seismicity.

Evidence clearly points to 3-D modelling as a need and not only a convenience.

4 STRAIN DISCONTINUITY MODEL

The model described here is called VOLSIM : volume simulation around mining. Features that are introduced in this paper are the strain discontinuity element, use of Fast Fourier Transforms (FFT's) to reduce computer run times, iteration through the Jacobi method with weighted averaging of neighbours and the implementation of suitable constitutive laws. Figure 3 is a block diagram of VOLSIM.

4.1 Strain Discontinuity elements

Peirce and Ryder (1983) presented results from an extended 2-D Boundary Element method for modelling the rock mass around deep-level mining excavations as a brittle continuum, based on work by Bannerjee and Cathie (1979) and Peirce (1983). Peirce and Ryder integrated point elements to form square elements rather than crack-like line elements. By filling the rock around square tunnels with these elements, they

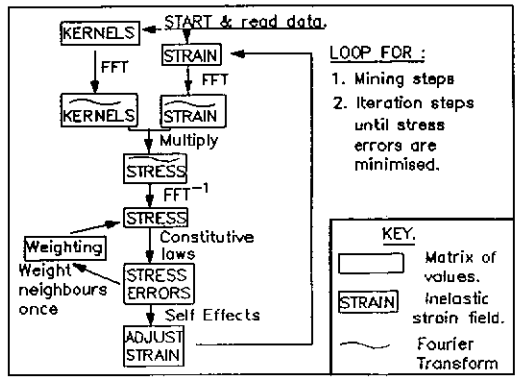

Fig. 3 A block diagram of VOLSIM.

were able to predict inelastic deformations that were in good qualitative agreement with observations. Peirce (1983) showed that models with large numbers of elements were more efficiently calculated using his Boundary Element method than could be achieved with the same accuracy using Finite Elements due to the times required to invert the large Finite Element matrices.

Peirce's elements represent a uniformly average, or piece-wise constant, inelastic strain change throughout each element : these elements are called STRAIN DISCONTINUITY elements here. Strain discontinuity elements are similar to Displacement Discontinuity elements in that they represent localised inelastic behaviour superimposed on an otherwise elastic material and an idealised deformation shape is associated with each element.

4.2 Use of FFT's

A central feature of the Boundary Element method is that stress values at any point in a mostly elastic rock mass can be determined from the sum of inelastic elements multiplied by influence kernels which are functions of elastic properties and geometric factors (Crouch and Starfield, 1983). The stress at any point ij can be expressed as

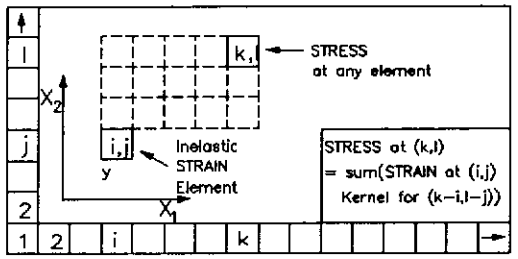

Fig. 4 Diagram illustrating the 2-dimensional geometry used by VOLSIM and the simple meaning of influence Kernels.

$$(\sigma_{mn})_{ij} = \sum (\epsilon_{op})_{kl} \cdot (c_{mnop})_{k-i,l-j}$$

where σ_{mn} are the three components of induced stress and ϵ_{op} are the three components of inelastic strain with mn and op = 11, 12 or 22, c_{mnop} is the influence coefficient function and i,j,k & l are element grid positions as shown for VOLSIM in Figure 4. Summation takes place over k & l. The influence coefficient in this simple geometry is a convolution operator and thus stress can be evaluated form inelastic strain using Fourier Transforms.

Following Stuart (1979) and Spottiswoode (1990), FFT's are used to reduce calculation of the stress from the inelastic strain field within the regular geometry of Figure 4 to $\tilde{N}\log_2 N$ from $\tilde{N}^2$ operations. As FFT's are more efficient in powers of two, the program was run using 16^2, 32^2 or 64^2 elements. Using an IBM-AT compatible computer running under MS-DOS and compiled in FORTRAN, VOLSIM uses 440 kiloBytes of memory.

4.3 Constitutive laws

While stopes were modelled with complete closure restriction, inelastic rock deformation took place using the Mohr-Coulomb failure criterion. Complete closure was limited by $\epsilon_{22} \leq S_w/g$, where S_w is the stope width and g is the element grid size.

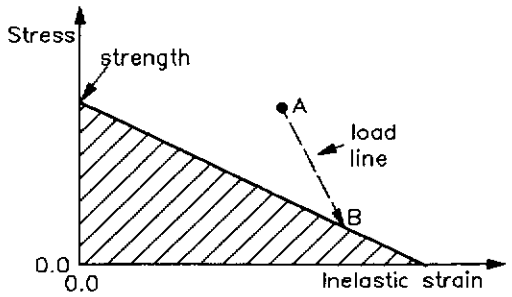

Fig. 5. Sketch showing weakening of rock strength with increasing inelastic strain. The shaded area is the residual strength.

Mohr-Coulomb failure with strain weakening was implemented as horizontal bedding-plane slip, slip on vertical joints or solid-rock failure. Solid-rock failure was allowed to take place on the more vertical of the two conjugate shear planes that are inclined at $45° - (\tan^{-1}\mu)/2$ to the maximum principal stress direction (Jaeger and Cook, 1976).

As strain softening behaviour can lead to numerical instability, strain weakening of rock strength for all elements was limited to a slope (stress divided by strain) of one quarter of the value of load line, or the self-effect kernel, as shown in Figure 5.

4.4 Iteration strategy

In the conventional Jacobi method, stresses are calculated from strains in one pass and stress errors are then converted to inelastic strain changes simultaneously at all elements. This process is repeated until stress errors are sufficiently reduced. Unfortunately, this method was found to lead to oscillatory or divergent behaviour in typical situations and strategies were sought to obtain stable and well controlled convergence. After some experimentation, two methods that resulted in relatively rapid, but still controlled, numerical behaviour were finally adopted.

Table 1. Matrix of weighting factors for adjusting errors on σ_{22}. m and n are relative addresses in the horizontal and vertical directions.

		m				
		2	1	0	1	2
	2			-.17		
	1		.09	-.53	.09	
n	0	.07	.34		.34	.07
	-1		.09	-.53	.09	
	-2			-.17		

Table 2. Geometry, elastic moduli and ambient stress conditions.

Element size	10 m by 10 m
Stope width	1 m
No. elements	32 by 32
Mining steps	16
Young's modulus	70 000 MPa
Poisson's ratio	0.2
Vert. stress	80 MPa
Hor. stress	40 MPa

Firstly, at each iteration step, the values of stress errors on failed elements were reduced by the maximum stress error on all mined elements. This removed the effect of the numerical stress wave that propagated during the iteration process from the newly mined elements towards the back areas.

Secondly, strain adjustments of adjacent elements, in the normal Jacobi scheme, interact strongly with one another and cause overdamped behaviour in some situations and underdamped behaviour in others. VOLSIM anticipated this behaviour by adjusting the stress residuals by a weighted average value of the stress residuals on 12 neighbours before applying the self-effect corrections to get strain changes. The weighting factors were simply the values of the influence kernels $(c_{mnop})_{ij}$ normalised by the self effect, with suitable signs, as illustrated in Table 1 for $(c_{2222})_{ij}$, which is used in calculating vertical stresses σ_{22} from vertical strains ϵ_{22}.

Weighting of neighbours using the positive values at $m \neq 0$ and $n = 0$ resulted in considerably faster solution convergence in mined areas than when no weighting took place. Negative weights also inhibited simultaneous solid-rock failure of adjacent elements and encouraged zonation.

5 RESULTS

Mining of the extensive tabular gold reefs typically takes place by development of an up-dip raise along reef for distances from 10 metres to 1000 metres, followed by ledging and then stoping in both directions, say East and West. Raises are typically spaced at distances of 160 m to more than 1000 m apart along strike. This system leads to simple mining geometries that are maintained as long as possible.

The complete cycle of mining from an infinite set of raises spaced 320 metres apart at a depth of 3 km below surface to remnant removal was simulated for this paper. Mining started with a 10 m wide raise and continued towards the East and West in 10m mining steps through to complete remnant extraction, with the entire area mined out in 16 mining steps. The mining geometry is shown in plan in Figure 6 and in section in Figure 7. Relevant mining parameters are listed in Table 2.

Four scenarios, number 1 to 4, were considered. As indicated in Table 3, the rock mass was not permitted to fail in scenarios 1 and 2. In scenarios 3 and 4, slip on pervasive sets of strong beds and joints was limited by a cohesive strength (C_0) of 10 MPa and a coefficient of friction (μ) of 1.0, while failure at other orientations was limited by $\sigma_{max} = 100\,MPa + 6.0 \cdot \sigma_{min}$. Weak beds and joints were inserted locally into scenarios 2 and 3 and extensively into scenario 4. The frictional

Table 3. Number of weak joints (J) and beds (B) for each of the four scenarios. Pervasive deformation of the rock mass (R) at all elements is allowed in scenarios 3 and 4.

	Presence of rock types		
Scenario	J	B	R
1	0	0	
2	1	3	
3	1	3	All
4	32	32	All

Table 4. Rock strength for "weak" and "strong" bedding and joint planes.

Type	Cohesion C_0, MPa	Friction μ
Weak	2.0	0.6
Strong	10.0	1.0

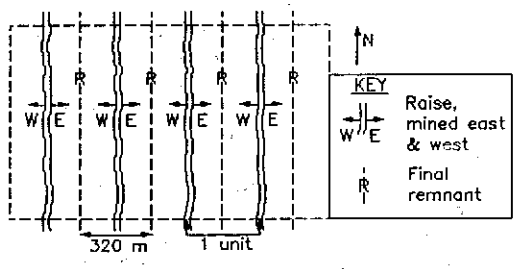

Fig. 6 Mining geometry in plan. The diagram indicates the infinitely repeating nature of VOLSIM.

properties of strong and weak beds and joints is listed in Table 4. The number of weak planes is summarised in Table 3 and their positions for scenarios 2 and 3 are shown in Figure 7.

The geometry of localised planes of weakness used for scenarios 2 and 3 is shown in section in Figure 7. Scenario 1 was the elastic case, with mining taking place in unfailing rock, while the rock mass was uniformly weak in scenario 4.

The distribution of inelastic strains in scenario 3 for mining spans of 210 and 270 metres is illustrated in Figure 8. At a span

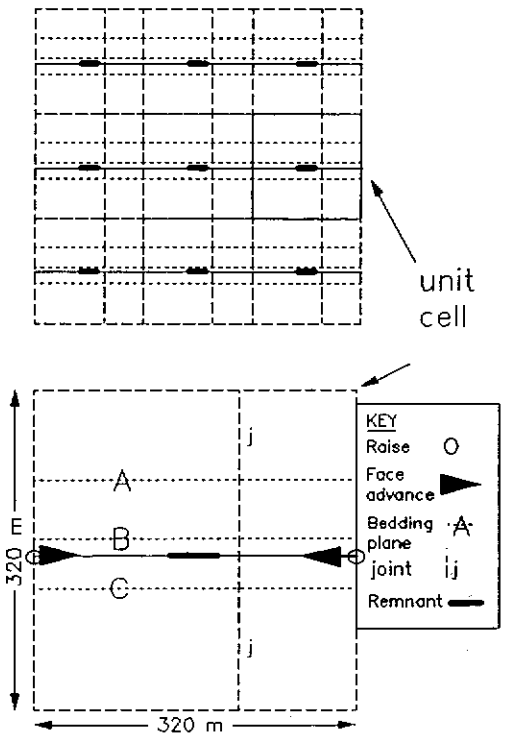

Fig. 7 Section through scenarios 2 and 3. VOLSIM models a unit cell within an infinitely repeating rock mass. Weak beds are labelled A, B and C.

of 210m, with 110m of unmined reef, slip occurred on the hangingwall and footwall sections of the weak ($\mu = 0.6$) joint and on the weak ($\mu = 0.6$) bed B, which also became connected to the stoping by deformation on two of the pervasive, but stronger ($\mu = 1.0$) joint zones. In all, six new linear failure zones, each some 70m long, developed.

At all spans, slip on bed B took place freely above the advancing stope, but reversed direction in the back areas as values of shear and normal stress reduced with further mining. The slip reversal stopped once complete closure took place. The mobilisation of bed C started at a span of 110m and resulted in failure of the stronger rocks between C and the stope when the span reached 170m.

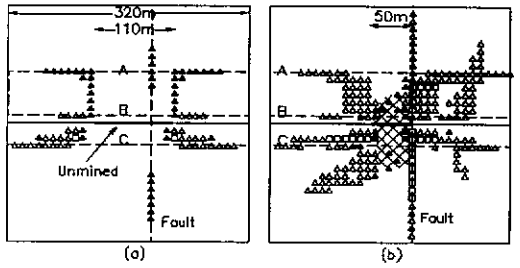

Fig. 8a and b. Distribution of shear deformation for scenario 3 at a span of (a) 210m and (b) 270m. Triangles indicate strain > 10^3 and squares, strain > 10^2. Empty symbols show that elements were first mobilised in a previous mining step, while solid symbols indicate freshly failed rock. The cross-hatched area in (b) shows deformation during extraction of the remaining 50m of reef. Beds are again marked A, B and C.

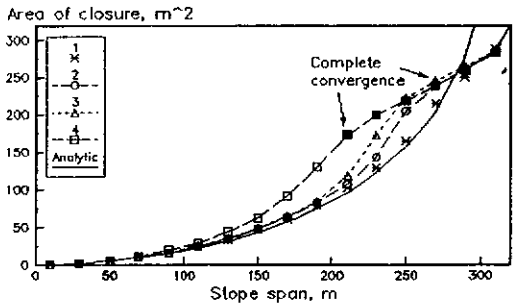

Fig. 9 Plot of stope closure as a function of the stope span.

Face advance through spans of 230m and 250m resulted in further fault and bedding slip as well as extensive zones of deformation of the strong, country rock, mostly between beds A and B and below bed C. Deformation took place both ahead of and behind the advancing face. Closure became complete in the back areas at a span of 250m (Figure 9) and inhibited further deformations above and below the stopes by reducing shear stresses.

At spans of 270m (Figure 8b) or more, additional rock deformation took place almost exclusively around the shrinking remnant. At a span of 270 m, a remnant 50m wide remains and the extraction ratio is 84 percent, close to the figure commonly used for designing layout for stabilising pillars (Ozbay and Ryder, 1989). Figure 8b is similar to the observations of Ozbay and Ryder as shown in Figure 2, if allowance is made for the effects of multi-step mining and mobilization of the weak beds and the joint in Figure 8b.

Mining of the remaining 50 metres of reef resulted in further deformation, generally more intense than before, but limited to a smaller volume of rock around the final remnant as indicated in Figure 8b.

The total area of stope closure $g^2 \sum \epsilon_{22}$ is shown in Figure 9 as mining progressed in all four scenarios. In the elastic case the curve followed the correct analytic shape until complete closure took place in the back areas. In the other scenarios, the country rock was allowed to deform more easily through shearing and the stope closed progressively more rapidly as weak zones were more easily mobilized.

A quantitative analysis of the total shear deformation is presented in Figure 10 in terms of γ as a function of stope span for the three inelastic models. γ is here the ratio of the summed change in shear deformation to the increase in stope closure within each model at each mining step. It can be seen that γ varies with geological conditions as expected, but that within each scenario it is not constant at all, increasing from zero to 0.6 for scenario 2, to 0.9 in scenario 3 and to 1.3 for scenario 4.

From considerations of scaling, the initial increase can be ascribed to non-zero values of cohesive strength and UCS. A more rapid increase in the value γ with increasing span was indeed obtained in an additional simulation in which the shear cohesive strength on all elements was reduced to zero and the UCS from 100 to 50 Mpa. Further reduction of the UCS to 25

MPa led to unstable behaviour numerical behaviour around the back areas for spans in excess of 130 m.

It is useful to convert the total shear deformation within each mining step to an equivalent seismic moment to estimate the magnitude of the largest expected seismic event during each step. For example, total shear slip on the joint in scenario 3 amounted to some 15m^2 in both the footwall and hangingwall. By assuming a strike length of 100m, using G = 3.10^{10} N-m and log M_0 = 1.5M + 9.1 (Hanks and Kanamori, 1979), two M=3.0 seismic events, above and below reef, could have resulted in this slip. This value is in reasonable agreement with the events with M=3.0 and M=3.3 that Lenhardt (1989) reported for a similar mining geometry.

The number of iteration steps for each mining step in VOLSIM was not more than twice the number of non-linear elements that deformed during each step, only exceeding 200 iterations when inelastic deformations were extensive. Run-times were some 10 seconds per iteration for the 32 by 32 problems analysed here on an IBM-AT compatible running at 12 MHz clock speed. Simulations of all four scenarios were completed in 12 hours of computer time. Run-times increased five-fold for runs of 64 by 64.

6 DISCUSSION

Convolutions obtained from Fourier transforms, as in this report, are subject to errors due to the circular nature of the convolution process as indicated by the repetition in Figures 6 and 7. As the modelled area is often similar to the surrounding areas in extensively mined regions, horizontal repetition has advantages as well as disadvantages. Interaction amongst the stopes repeated in a vertical sense is minimal, but inelastic deformations extending into the hangingwall and footwall interact strongly as they each approach

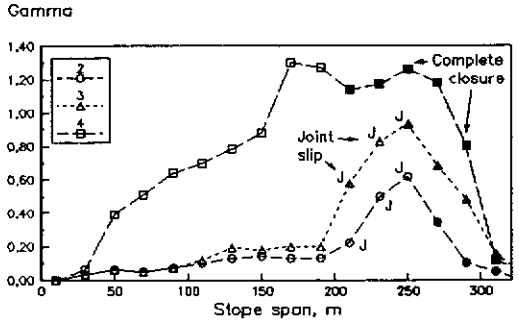

Fig. 10 Plot of γ as a function of the stope span.

their common border.

To test errors introduced by circular convolution, stoping within scenario 3 was duplicated horizontally within a 64 by 64 model, while rock-mass characteristics were extended vertically to the new boundaries to reduce the effect of interaction in a vertical sense. Off-reef deformations in the 64^2 model were found to lag behind those of the 32^2 model by up to ½ a mining step. The maximum cumulative shear deformation took place at a span of 290m in both cases, but was 12 percent less for the 64^2 model. Errors introduced by circular convolution in mining geometries with numerous remnants and/or areas of complete closure would probably be less than 10 percent in most cases. Stress gradients due to the effect of gravity do not pose numerical problems.

Figure 10 illustrates that changed rock properties can have a major effect on the total amount of shear slip, in agreement with Webber (1990). This effect was particularly apparent for spans between 50m and 200m, but lessened at greater spans once complete convergence took place and as stresses increased around the final remnant. The same results would be expected if different ambient stress conditions were assumed.

The pervasive fracturing around deep-level stopes has been mimicked reasonably well here, both qualitatively and quantitatively, in 2-D. A 3-D version of VOLSIM has

already been written for elastic behaviour of the rock mass. It is planned to extend it to include inelastic deformations around realistic mining geometries, including those previously subjected to MINSIM-D ESS studies. Without special optimization, a full 64^3 3-D version needs about 25 MBytes of RAM. A CPU speed of about 10 million floating points per second (MFlops) will be needed to keep to reasonable run-times of, say, less than 24 hours. VOLSIM could readily be optimised to take advantage of parallel processing capabilities, both by using appropriate FFT algorithms and while calculating constitutive behaviour.

At this stage, VOLSIM has not been compared in detail to results obtained by other models. The work to date has been done from the perspective of a seismologist to obtain reasonable values of γ and seismicity over a complete mining cycle. This has been reasonably successful even though the details of the deformations close to the advancing face have been neglected.

Much work must still be done on the 2-D version, particularly regarding the rock failure behaviour close to the face where stress and strain gradients are at a maximum. A higher-order element placed immediately ahead of the advancing face might remove the inability of VOLSIM to recognize that the face crushes. Such an element would have zero average inelastic strain, but could introduce asymmetrical and intense interaction with immediate neighbours. Higher-order elements might seem somewhat contrived, but their value could be tested in a simple fashion by placing a suitable element within a vertical plane with zero strength and frictional properties to simulate a plane of symmetry.

Some work has been done on the concept of Fourier kernels, obtained from the integral Fourier transform of kernels derived from point strain discontinuities. Point strain discontinuities fortunately transform to very simple functions, but rejection of the short wavelengths using a simple box-car filter in the wavenumber domain results in strong Gibb's effects (Bracewell, 1965) in the spatial domain. These effects appear as strange oscillations of the close-in kernel coefficients in the spatial domain. Preliminary work using Fourier Kernels indicates that strain energies obtained through volume integration are nearly identical to those obtained from stope closure, whereas errors of the order of 10 percent are introduced using piece-wise constant strain kernels, presumably due to errors at short wavelengths introduced at the edges of these kernels. Perhaps Fourier kernels could be filtered to optimise the spatial behaviour while still maintaining their advantages at short wavelengths.

γ has been defined in this report in terms of total shear deformation, including the bedding-plane slip that took place tens of metres in the back areas. As significant seismicity rarely takes place in the back areas, unless associated with major geological features, we need constitutive laws that can differentiate between seismic and aseismic deformation.

Seismicity during longwall mining has been correlated with ERR values up to 100 MJ/m^2 since the 60's (Anon, 1988). However, remnant extraction can take place at ERR values in excess of 200 MJ/m^2 without resulting in intense seismicity (Spottiswoode, 1988). The reduced level of seismicity is well modelled by the decrease in γ shown in Figure 10. The more intense fracturing around the final remnant, without preference to geological planes of weakness (Figure 8b) is also in agreement with the change in character of microseismicity during remnant extraction documented by Legge and Spottiswoode (1987). They suggested that seismological "b"-values of 1.5 were a manifestation of failure spreading within a volume of rock

without preference to discrete planes. Only 3-D deformation can account for both Figure 8b and the microseismic behaviour.

7 CONCLUSIONS

This paper presents a new numerical model capable of simulating the intensive, extensive and pervasive deformations that take place around deep-level tabular excavations. Plane-strain simulations of a complete cycle of mining starting from raises spaced 320m apart at 3 km depth through to final remnant extraction showed deformations that were in good qualitative and quantitative agreement with observations :

1. The rock mass deformed extensively, even for coefficients of friction as high as 1.0.
2. Weaker beds and joints, with coefficients of friction of 0.6, were mobilized widely and preferentially until a remnant 50m wide had been formed, after which intact rock failed pervasively within a more limited volume.
3. Shear slip on joints with reduced coefficients of friction could have formed the source region of M=3 seismic events.
4. The seismological parameter, γ, was found to increase with increasing span to values of around 1.0 and then to decrease during the final remnant removal.

The following points arise from the paper and the current status of VOLSIM :

1. Its performance has not been directly compared against programs using Finite Element or Discrete Element methods. Comparisons are needed particularly for the demanding mining situations modelled in this paper.
2. It needs a face crushing element.
3. The application of further constitutive laws should be investigated, as should a method to distinguish seismic from aseismic deformations.
4. The role of Fourier transforms in the method used here, and the potential for further application, needs to be better investigated and presented to the Rock Engineering fraternity.

8 ACKNOWLEDGEMENTS

The author is grateful for discussions at the Chamber of Mines Research Organization (COMRO) with many with a deeper knowledge of numerical modelling, particularly Drs JAL Napier and JA Ryder. Dr AP Peirce has provided us with mathematical insights into Fourier kernels. Thanks to Dr MU Ozbay for discussions on the original samples from which Figure 2 was drawn. This paper benefited from numerous suggestion by Drs JAL Napier and NC Gay. It forms part of the work done by COMRO for the South African gold mining industry and permission to publish is gratefully acknowledged.

9 REFERENCES

Anon 1988. An industry guide to methods of ameliorating the hazards of rockfalls and rockbursts - 1988 edition. Research Organisation, Chamber of Mines of South Africa.

Aki, K. 1981. A probabilistic synthesis of precursory phenomena. Earthquake Prediction - International Review : 566-574, Maurice Ewing Volume, Amer. Geophys. Union.

Bannerjee, P.K. and Cathie, D.N. 1979. A direct formulation and numerical implementation of the boundary element method for two dimensional problems of elasto-plasticity. Int. J. Mech. Sci., 22 : 238-245.

Bracewell, R.N. 1965. The Fourier Transform and its application. McGraw-Hill.

Brummer, R.K. and Rorke, A.J. 1990. Case studies on large rockbursts in South African Gold Mines. Proceedings of the Second International Symposium on Seismicity In Mines, Minnesota, USA. In press.

Crouch, S.L. and Starfield, A.M. 1983. Boundary element methods in solid mechanics. George Allen & Unwin.

Gay, N.C. 1979. The state of stress in a large dyke on E.R.P.M., Boksburg, South Africa. Int. J. Rock Mech. Min. Sci. & Geomech. Abstr. 16 : 179-185.

Hanks, T.C. and Kanamori, H. 1979. A moment magnitude scale. J. Geophys. Res. 84 : 2348-2350.

Jaeger, J.C. and Cook, N.G.W. 1976. Fundamentals of Rock Mechanics, 3rd edition. Chapman and Hall, London.

Lenhardt, W.A. 1989. Seismic event characteristics in a deep-level mining environment. Proceedings, ISRM-SPE Int. Symp. on Rock at Great Depth, Pau France : 527-535.

Legge, N.B. and Spottiswoode, S.M. 1987. Fracturing and microseismicity ahead of a deep gold mine stope in the pre-remnant and remnant stages of mining. Proceedings of the Sixth International Congress on Rock Mechanics, Montreal, Canada : 1071-1077.

McGarr, A. 1976. Seismic moments and volume changes. J Geophys. Res. 81: 1487-1494.

McGarr, A. and Wiebols, G.A. 1977. Influence of mine geometry and closure volume on seismicity in a deep-level mine. Int. J. Rock Mech. Min. Sci. & Geomech. Abstr. 14: 139-145.

McGarr, A. 1986. Some comments on the nature of Witwatersrand mine tremors. Unpublished report.

Mandelbrot, B.B. 1983. The fractal geometry of nature. WH Freeman, New York.

Ortlepp, W.D. 1978. The Mechanism of a Rockburst. Proceedings of the 19th U.S. Rock Mechanics Symposium, University of Nevada, Reno : 476-483.

Ozbay, M.U. and Ryder, J.A. 1989. Investigations into foundation failure mechanisms of hard rock squat rib pillars. Proceedings, ISRM-SPE Int. Symp. on Rock at Great Depth, Pau France : 527-535.

Peirce, A.P. 1983. The applicability of the non-linear boundary element method in the modelling of mining excavations. Unpublished MSc dissertation, University of the Witwatersrand, Johannesburg.

Peirce, A.P. and Ryder, J.A. 1983. Extended boundary element methods in the modelling of brittle rock behaviour. Proceedings of the Fifth Congress of Int. Soc. of Rock Mech., Melbourne. F159-F167.

Ryder, J.A. 1988. Excess shear stress in the assessment of geologically hazardous situations. J.S.Afr. Inst. Min. Metall. 88: 27-39.

Ryder, J.A. and Napier, J.A.L. 1985. Error analysis and design of a large-scale tabular stress analyser. Proceedings of the Fifth International Conference on Numerical Methods in Geomechanics. Nagoya, Apr. 1549-1555.

Spottiswoode, S.M. 1984. Source mechanisms of mine tremors at Blyvooruitzicht Gold Mine. Proceedings of the First International Symposium on Rockbursts and Seismicity in Mines, Johannesburg, S. Afr. Inst. of Min. Metall : 29-37.

Spottiswoode, S.M. 1988. Total seismicity, and the application of ESS analysis to mine layouts. J. S. Afr. Inst. Min. Metall. 88: 109-116.

Spottiswoode, S.M. 1990. Volume Excess Shear Stress and cumulative seismic moments. Proceedings of the Second International Symposium on Seismicity In Mines, Minnesota, USA. In press.

Stuart, A.D. 1979. An application of the Fast Fourier Transform in numerical elasticity. MSc Thesis, University of the Witwatersrand.

Webber, S.J. 1990. Numerical modelling of repeated fault slip. Submitted to J. S. Afr. Inst. Min. Metall.